

Jun-Young Park · Eric D. Wachsman

Stable and high conductivity ceria/bismuth oxide bilayer electrolytes for lower temperature solid oxide fuel cells

Received: 6 February 2006 / Accepted: 10 February 2006 / Published online: 25 April 2006
© Springer-Verlag 2006

Abstract A highly conductive bismuth oxide/ceria bilayer electrolyte was developed to reduce solid oxide fuel cell (SOFC) operating temperatures. Bilayer electrolytes were fabricated by depositing a layer of $\text{Er}_{0.2}\text{Bi}_{0.8}\text{O}_{1.5}$ (ESB) of varying thickness via pulsed laser deposition and dip-coating on a $\text{Sm}_{0.2}\text{Ce}_{0.8}\text{O}_{1.9}$ (SDC) substrate. The open-circuit potential (OCP) and ionic transference number (t_i) of ESB/SDC electrolytes were tested in a fuel cell arrangement as a function of relative thickness, temperature, and P_{O_2} with $\text{H}_2/\text{H}_2\text{O}$ and CO/CO_2 on the anode side and air on the cathode side. These EMF measurements showed a significant increase in OCP and t_i with the bilayer structure, as compared to the cells with a single SDC electrolyte layer. Furthermore, improvement in the OCP and t_i of bilayer SOFCs was observed with increasing relative thickness of the ESB layers. Hence, the bilayer structure overcomes the limited thermodynamic stability of bismuth oxides and prevents electronic conductivity of ceria-based oxides in reducing atmosphere.

Keywords Solid oxide fuel cells · Low temperature SOFC · Bilayer electrolytes · Ceria · Bismuth oxide

Introduction

Solid oxide fuel cells (SOFCs) efficiently generate electricity electrochemically with negligible emissions [1]. Furthermore, SOFCs provide many desirable characteristics: high reliability, durability, vibration-free operation, and fuel versatility. Reduction of the operating temperature would allow the use of low-cost and durable sealants and interconnects. Operating SOFCs below 800 °C (intermediate temperature, IT) would also yield faster start-up times for portable use, increase efficiency and stability, and diminish excessive power consumption for reaching and

operating the SOFC at high temperature. This has driven the development of IT-SOFCs in recent years [2, 3]. Extending this development to even lower temperature (<600 °C) could potentially open up the transportation and portable power markets to SOFCs.

One major issue in the improvement of the performance of lower temperature SOFCs is the development of a solid oxide electrolyte (SOE) with sufficiently high ionic conductivity [4, 5]. Alternative SOEs, such as samaria-doped ceria (SDC) and erbia-stabilized bismuth oxide (ESB), have been suggested because their conductivity is one to two orders of magnitude higher than that of current yttria-stabilized zirconia (YSZ) electrolytes [6, 7]. In spite of the high conductivity of ESB, it has not been used in SOFCs due to its limited thermodynamic stability. ESB decomposes to metallic bismuth in the presence of a reducing agent (fuel gases) [8]. Therefore, to use ESB as an SOE, exposure to reducing atmosphere must be prevented. Samaria-doped ceria (SDC) has received greater attention as a potential IT-SOE due to its high ionic conductivity and phase stability at low-oxygen partial pressure (P_{O_2}) [9]. However, SDC becomes a mixed ionic-electronic conductor (MIEC) at low P_{O_2} (< 10^{-14} atm), exhibiting considerable n-type electronic conduction through the electrolyte [10]. This phenomenon decreases the ionic transference number (t_i) with lower open-circuit potential (OCP), thereby reducing the SOFCs efficiency. It is, therefore, crucial to increase the stability and electrolytic domain of these materials to limit electronic conduction.

Bilayer electrolytes can be used to increase the thermodynamic stability of ESB and SDC [11–13]. However, in most of these investigations YSZ was used to protect these high conductivity materials from reduction by avoiding exposure of the reducing gas [11, 12]. In contrast, our bilayer electrolytes consist of SDC on the reducing side and ESB on the oxidizing side [13]. In a functionally graded ESB/SDC bilayer structure (Fig. 1), the gradient of P_{O_2} is determined by the gas phase on either side and the relative ionic and electronic conductivity of each layer. The P_{O_2} at the ESB/SDC interface can be controlled (to avoid ESB

J.-Y. Park · E. D. Wachsman (✉)
Department of Materials Science and Engineering,
University of Florida,
Gainesville, FL 32611, USA
e-mail: ewach@mse.ufl.edu

reduction) by varying the thickness ratio of SDC and ESB layers. Thus, thermodynamic stability of the ESB can be maintained if the ESB is never exposed to an interfacial P_{O_2} lower than the decomposition P_{O_2} . Thus, relative thickness is a key parameter to the electrochemical performance of bilayer electrolytes. Also, higher t_i with increased OCP can be obtained in bilayer ESB/SDC electrolytes than with single SDC electrolytes, as the ESB layer serves to block electronic flux through the electrolytes.

We previously demonstrated that an ESB/SDC bilayer electrolyte is stable and obtains a higher OCP and power density than an SDC electrolyte SOFC [13]. Furthermore, our concept predicts that the stability and OCP should depend on the relative thickness of the ESB and SDC layers. Therefore, the primary objective of this study is to confirm our bilayer concept by demonstrating the effect of relative thickness on OCP and t_i . In this work, bilayer ESB/SDC SOFCs are investigated as a function of relative thickness and anode P_{O_2} under open-circuit conditions, and compared to the single-layer SDC electrolyte SOFCs.

Experimental description

SDC sample preparation

SDC ($\text{Sm}_{0.2}\text{Ce}_{0.8}\text{O}_{1.9}$) samples were prepared from polycrystalline powders of ceria (99.99%) and samaria (99.9%) obtained from a commercial source (Alfa Aesar). The desired electrolyte composition was prepared by the conventional solid-state synthesis technique. The powder was mechanically milled with zirconia media in ethanol for 24 h, calcined at 1,200 °C for 10 h, pulverized, and sieved. SDC powders were compacted uniaxially, subsequently pressed isostatically, and sintered at 1,600 °C for 10 h, forming pellets 2.5 cm in diameter and 0.2 cm in thickness. The relative density of the SDC disks was found to be more than 98% using Archimedes method.

Preparation of thin and thick films by PLD and dip-coating

ESB thin films were deposited on one side of polished SDC substrates via pulsed laser deposition (PLD). The ESB

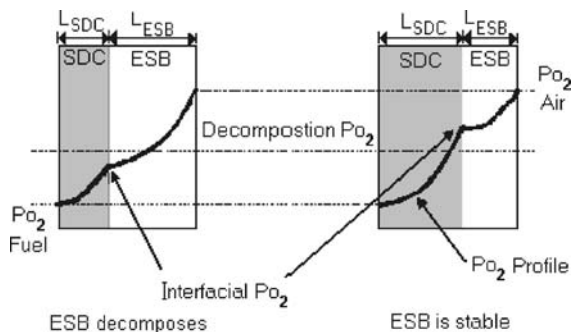


Fig. 1 Conceptual representation of a bilayer electrolyte showing the effect of relative thickness on interfacial oxygen partial pressure (P_{O_2})

($\text{Er}_{0.2}\text{Bi}_{0.8}\text{O}_{1.5}$) target synthesis procedure was similar to that described above for SDC. During PLD, the ESB target was rotated, the KrF excimer laser (Lambda Physik LPX 305 i KrF excimer laser) frequency was set at 10 Hz, and the laser energy was 500 mJ, yielding a substrate temperature of 700 °C. The thickness of the ESB film was less than 1.5 μm by profilometry (Alpha-step 500, Tencor) in this work.

ESB/SDC bilayer electrolytes were also fabricated by the dip-coating [14] technique to make thicker ESB films. For dip-coating, ESB powder was prepared by the citrate process [15] using stoichiometric amounts of $\text{Bi}(\text{NO}_3)_3 \cdot x\text{H}_2\text{O}$ (99.999% pure, Alfa Aesar) and $\text{Er}(\text{NO}_3)_3 \cdot 5\text{H}_2\text{O}$ (99.99% pure, Alfa Aesar). An isopropanol suspension containing a small amount of ESB powder (5, 7, 10 wt%) was used to coat the SDC substrate. The dipping cycle was repeated to obtain the desired thickness and to reduce porosity of the electrolyte. The film-coated bilayer electrolytes were sintered at 890 °C for 10 h. Using three different concentrations of the ESB solution, the final film thicknesses were 9 to 30 μm by SEM (JSM-35CF JEOL) micrographs. Any other phases due to the interdiffusion between SDC and ESB were not detected by EDX and XRD (Philips APD 3720) of the samples. The fabrication and characterization of ESB/SDC bilayer electrolytes is described in detail in [16].

Electrode preparation

Platinum (Pt, Heraeus, CL11-5349) electrode pastes were applied on the SDC anode side. Pt reacts with ESB; therefore, gold paste (Au, Engelhard, HC1105) and Ag-ESB electrodes were deposited onto cathode sides of single-layer SDC electrolytes and the ESB side of bilayer electrolyte samples. As Au is a poor electrocatalyst for IT-SOFC operation, Ag-ESB was prepared and compared to the Au cathode. To form electrode inks, 50 vol.% Ag powders (99.9%, APS 0.5–1 μm , Alfa Aesar) and 50 vol.% ESB powders prepared using the citrate process, mixed in ethanol using mortar and pestle after adding solvent (α -terpineol), plasticizer (dibutyl phthalate), and binder (polyvinyl butyral). The slurries of electrode materials were then screen-printed onto the bilayer ESB/SDC electrolytes, dried at 125 °C for 30 min, and sintered at 800 °C for 1 h. Au, Pt, and Ag wires were then attached to the Au, Pt, and Ag electrodes, respectively, dried, and sintered under the same conditions as the electrodes to ensure good contact between electrodes and current collectors.

Measurement of OCP and t_i

Three types of SOFC designs were fabricated to verify the hypothesis that bilayer ESB/SDC electrolytes exhibit higher OCP than single-layer SDC or ESB electrolytes, to estimate the effect of thickness ratios of the bilayer electrolyte samples, and to investigate the effect of cathode performance on OCP and t_i .

Fig. 2 Experimental setup of fuel cell reactor using glass o-rings for sealing of gas

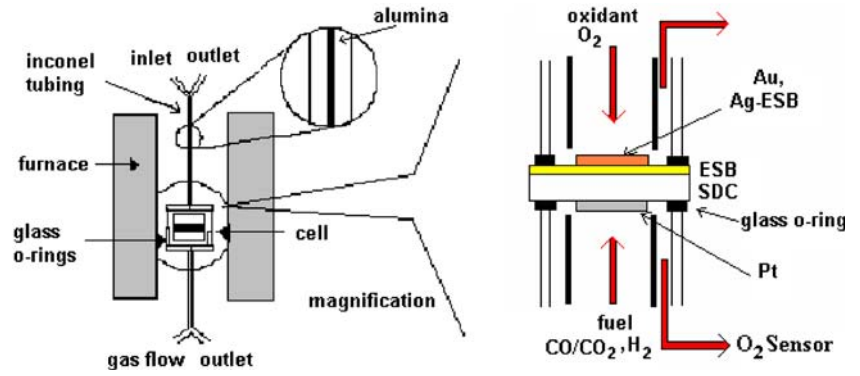
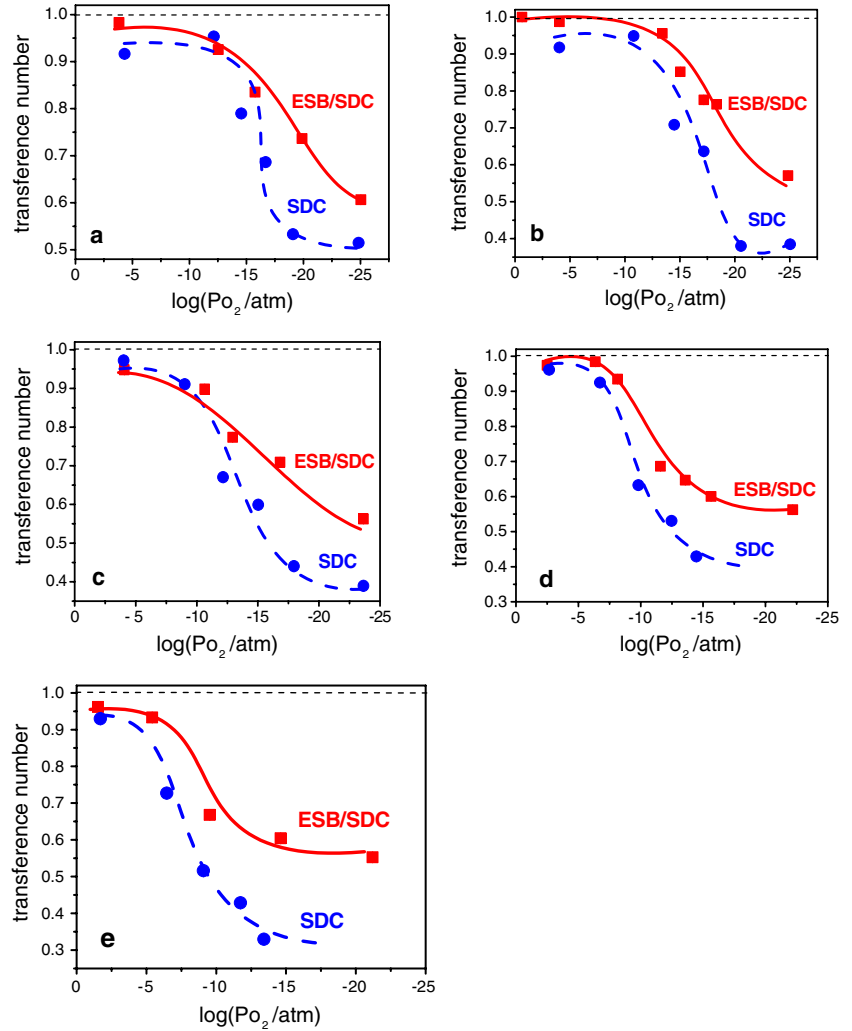


Fig. 3 Comparison of t_i of a single-layer SDC and bilayer ESB/SDC SOFC as a function of P_{O_2} at **a** 600, **b** 650, **c** 700, **d** 750, and **e** 800 °C



P_{O_2} , Au|SDC|Pt, P_{H_2/H_2O} or P_{CO/CO_2} [Cell I]

P_{O_2} , Au|ESB|SDC|Pt, P_{H_2/H_2O} or P_{CO/CO_2} [Cell II]

P_{O_2} , Ag-ESB|ESB|SDC|Pt, P_{H_2/H_2O} or P_{CO/CO_2} [Cell III]

Each bilayer substrate was identified as 0.8, 1.3, 9, 22, and 30 ESB/SDC, depending on the thickness of ESB layer

in micrometer, which was confirmed by profilometry and SEM analysis.

The experimental setup is shown in Fig. 2. The reactor was made of Inconel to avoid severe oxidation at high temperature. A long narrow Al_2O_3 tube was inserted in the Inconel tubing to prevent electrical short-circuit by isolating the gold wire from the metal tubing. The flow of gases into the reactor was regulated by calibrated mass flow controllers (Edwards 825, series B). The OCP of each

Table 1 Relative thicknesses of ESB/SDC electrolytes

Electrolytes	SDC layer thickness (mm)	ESB film thickness (μm)	Relative thickness (ESB/SDC)	Fabrication method	Cathode
0.8 ESB/SDC	1.60	0.8	5.0×10^{-4}	PLD	Au
1.3 ESB/SDC	1.76	1.3	7.4×10^{-4}	PLD	Au
9 ESB/SDC	1.5	9	6.0×10^{-3}	Dip-coating	Au
22 ESB/SDC	1.5	22	0.015	Dip-coating	Ag-ESB
30 ESB/SDC ^a	1.0	30	0.03	Dip-coating	Au

^aRelative thickness from previous results (from Wachsman et al. [13])

concentration cell was measured by a multimeter (Keithley Model 2000) under identical conditions over the temperature range 500–800 °C with a gas flow rate of 60 sccm. In the present measurements, the P_{O_2} was fixed at 0.21 atm (using air) on the SOFC cathode side. The OCP was obtained as a function of P_{O_2} (10^{-2} – 10^{-30} atm) on the anode side using various CO/CO₂ mixtures and H₂/H₂O (H₂ bubbling through room temperature H₂O). The anode P_{O_2} was taken to be that measured upstream by a zirconia oxygen sensor, assuming ideal gas-mixing conditions to hold in the reactor. The theoretical OCP can be attained only with no gas leak, either across the electrolyte or to the external atmosphere. Glass o-rings were used to prevent gas leak in the entire assembly. SDC and bilayer ESB/SDC electrolytes, were placed between rings of borosilicate (KG-33, Reelevs Glass). The entire assembly was inserted into the reactor as shown in Fig. 2. The assembly was heated to 900 °C at a ramp rate 3 °C/min and was cooled back down to operating temperature (500–800 °C) at the same rate. This technique allowed the glass to soften and made use of sealing the electrolyte and reactor tubing during of this work. Details on equipment fabrication may be found in [17].

Results and discussion

Comparison of OCP and t_i between SDC and ESB/SDC electrolytes in CO/CO₂ atmosphere

The OCP of the oxygen concentration cells described above were measured as a function of anode P_{O_2} (set by a CO/CO₂ ratio) and temperature to calculate t_i . Measured SOFC OCP was then divided by the OCP measured with a zirconia oxygen sensor (both referenced to air) to calculate t_i . The bilayer 1.3 ESB/SDC sample (ESB thickness 1.3 μm and SDC thickness 1.76 mm) was tested to verify the bilayer concept under these conditions.

Figure 3 compares t_i , obtained for single-layer SDC (Cell I) and bilayer ESB/SDC (Cell II) SOFC. At high anode P_{O_2} , the t_i of SDC and ESB/SDC cells were comparable and approached unity. However, at low P_{O_2} , n-type conduction developed due to reduction of ceria and resulting increase in the number of conductive electrons. The t_i of the ESB/SDC cell was greater than that of SDC

cell at every temperature and P_{O_2} of operation, and the difference was greatest at low P_{O_2} , where SDC by itself has the greatest n-type conduction. This enhancement in t_i is due to the ability of the ESB layer to block electronic flux, confirming the bilayer concept. Overall, the t_i of the cells decreased with increasing temperature as a result of the diminishing ionic domain of the SDC electrolyte.

It is important to note that CO/CO₂ gas mixtures were used to control the P_{O_2} . However, CO/CO₂ is known for not readily attaining equilibrium in these conditions with the electrodes used. Hence, very low OCP and t_i values

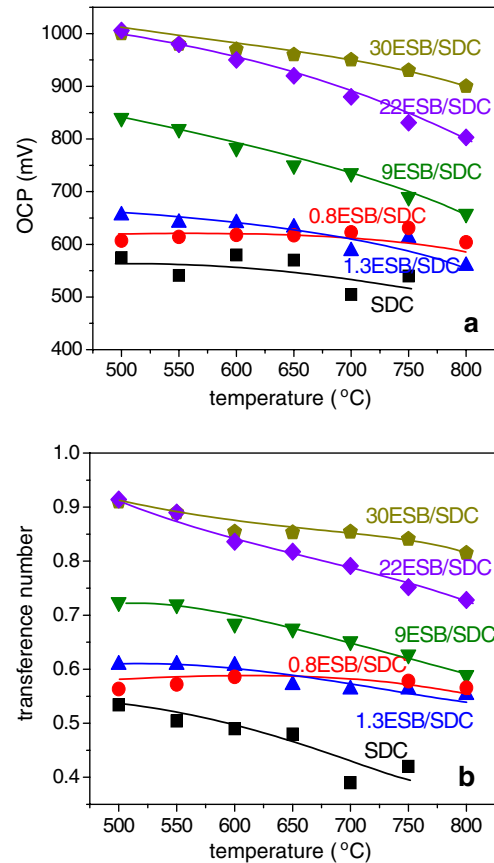


Fig. 4 Electrochemical performance of SDC and ESB/SDC electrolytes, **a** open-circuit potential (OCP) and **b** ionic transference number (t_i) as a function of temperature with air cathode and H₂/H₂O anode

were obtained from the experiment. Nevertheless, the improvement in OCP and t_i shown by the bilayer electrolytes is not obviated as all the cells were tested under the same conditions.

Effect of relative thickness in H₂/H₂O atmosphere

To investigate the effect of the relative thickness of bilayer ESB/SDC electrolytes on OCP and t_i , five cells were prepared by depositing ESB layers via PLD and dip-coating of varying thickness on identical SDC substrates. Table 1 shows the relative thickness of the ESB/SDC electrolytes.

Figure 4 summarizes the comparisons of the OCP and t_i for single-layer SDC and bilayer ESB/SDC electrolytes as a function of temperature for these relative thicknesses of ESB/SDC. In this paper, the P_{O_2} was maintained by H₂/H₂O on the anode and air on the cathode. The OCP and t_i increase as the ESB layer thickness increases. The 30 ESB/SDC cell resulted in the largest increase in OCP and t_i , compared to the uncoated SDC cell. The OCP of 30 ESB/SDC is 1,006 and 900 mV at 500 and 800 °C, respectively. The decrease in OCP and t_i with increasing temperature is due to the reduced ionic domain of the ceria electrolyte, as

mentioned in the previous section. The OCP and t_i of 30 ESB/SDC show small deviations from theoretical values, indicating a thicker ESB layer is necessary to achieve full theoretical OCP.

The OCP and t_i of ESB/SDC cells, as a function of relative thickness, are shown in Fig. 5. ESB/SDC cells result in a notable increase in OCP and t_i at all temperatures, compared to the single SDC cell, and the OCP and t_i increase with relative thickness of ESB. Specifically, as the thickness ratio (L_{ESB}/L_{SDC}) increases we observe that the OCP approaches the theoretical (Nernst) value and t_i approaches unity, consistent with our proposed concept. Furthermore, higher values of OCP and t_i approaching unity should be possible with further increase in the relative ESB/SDC thickness.

Effect of cathode

For comparison, a two-phase cathode consisting of Ag (an electrocatalyst and an electronic conductor) and ESB for ionic conduction was used on one cell. Fig. 6 shows typical surface and cross-sectional images of an Ag-ESB electrode on an ESB electrolyte. The Ag and ESB particles appear to have sintered well with each other and bonded well at the Ag-ESB/ESB interface. The morphology of the ESB differs in that the particles have rounded edges and are smaller in size, compared to those of Ag powder.

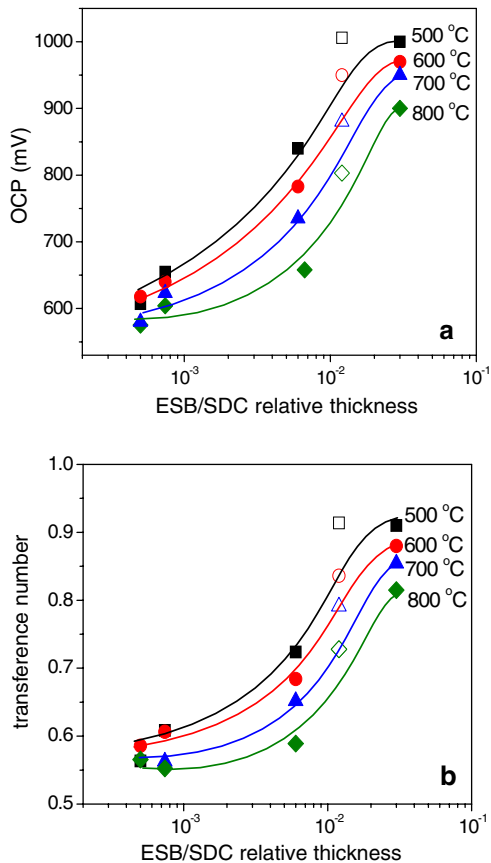


Fig. 5 Effect of ESB/SDC relative thickness and cathode on a OCP and b t_i relation of bilayer electrolyte SOFC with air on the cathode side and H₂/H₂O on the anode side (open symbol Ag-ESB cathode, and closed symbol Au cathode)

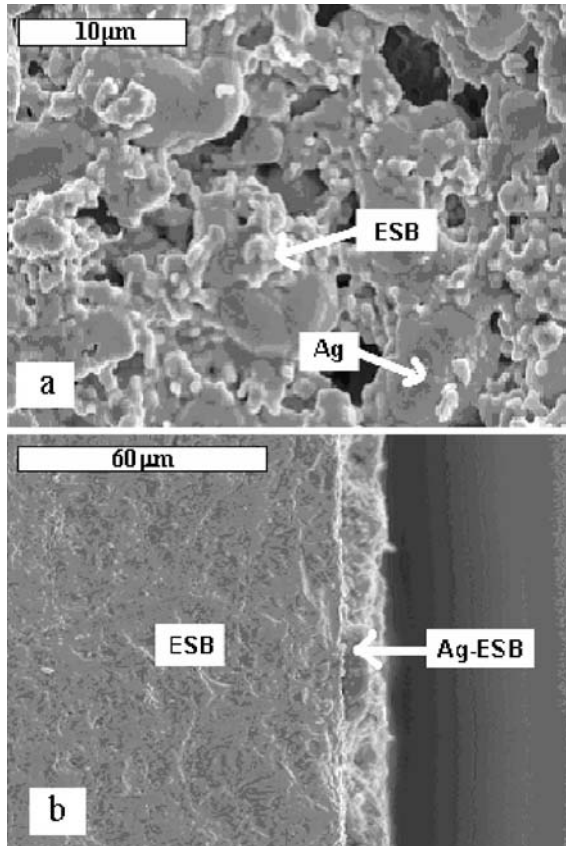
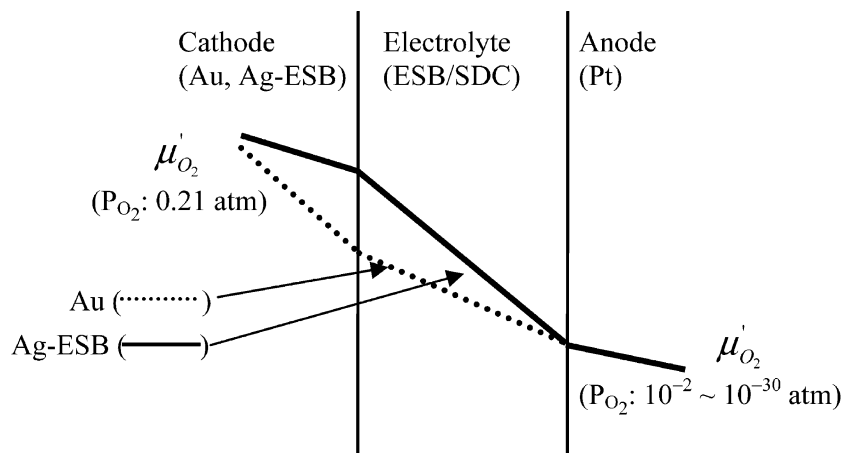


Fig. 6 SEM (a) surface and (b) cross-section images of Ag-ESB composite electrode on ESB substrate

Fig. 7 Effect of electrode overpotential on the variation of chemical potential of oxygen species across a SOFC with an Au and Ag-ESB cathode across the concentration cell



The electrochemical performance and OCP of SOFCs are influenced greatly by the characteristics of the cathode. In Fig. 5, OCP and t_i of SOFCs with Au and Ag-ESB cathodes, respectively, are represented by the closed and open dots. The OCP and t_i values of the ESB/SDC bilayer SOFC with the Ag-ESB cathode deviates from the sigmoidal shaped curve and shows higher OCP and t_i for that relative ESB/SDC thickness, which is a consequence of the reduced cathode overpotential. As Ag-ESB is a significantly better cathode than Au, its cathode overpotential is less; thus, the difference in chemical potential across the electrolyte with Ag-ESB cathodes is greater than with the Au cathodes (Fig. 7). Accordingly, a higher electrochemical potential (and t_i) was obtained for the ESB/SDC SOFC that had an Ag-ESB, rather than an Au cathode. Further improvement in the cathode should further increase the OCP and t_i of our bilayer ESB/SDC cells.

Conclusions

Bilayer electrolytes of various relative thicknesses were fabricated by depositing thin and thick films of ESB on SDC substrates by PLD and dip-coating. Measurements of the OCP and t_i in fuel cell construction of SDC and ESB coated with SDC were carried out. Due to blocking of electronic transport by the ESB layer, the bilayer ESB/SDC electrolyte exhibited a significantly higher OCP than those fabricated from a single-layer SDC electrolyte at all temperatures under the same conditions, and t_i of the bilayer electrolytes was higher than that of uncoated SDC electrolytes. Furthermore, the OCP and t_i of the bilayer ESB/SDC electrolytes increased with increasing relative ESB thickness. The increase in OCP and t_i of the bilayer cells is influenced by the ionic and electronic transport

properties of the two layers, their relative thickness, and the interfacial oxygen partial pressure. We expect even higher OCP and t_i values with thicker ESB and optimized electrodes in the near future.

Acknowledgements This work was supported by the U.S. Department of Energy under Contract #DE-AC26-99FT40712 and the U.S. Department of Energy High Temperature Electrochemistry Center at the University of Florida.

References

1. Singhal SC (2000) *Solid State Ionics* 135:305
2. Shahibzada M, Steele BCH, Helligardt BCH, Barth D, Effendi A, Mantzavinos D, Metcalfe IS (2000) *Chem Eng Sci* 55:3077
3. Torrens RS, Sammes NM, GA (1998) *Tompsett, Solid State Ionics* 111:9
4. JR Jurado (2001) *J Mater Sci* 36:1133
5. BCH Steele (2001) *Solid State Ionics* 129:95
6. Inaba, H Tagawa (1996) *Solid State Ionics* 83:1
7. Huang W, Shuk P, Greenblatt M (1998) *Solid State Ionics* 113:305
8. Wachsman ED, Ball GR, Jiang N, Stevenson DA (1992) *Solid State Ionics* 52:213
9. Yahiro H, Eguchi Y, Eguchi K, Arai H (1988) *J Appl Electrochem* 18:527
10. Eguchi K, Setoguchi T, Inoue T, Arai H (1992) *Solid State Ionics* 52:165
11. Virkar AV (1991) *J Electrochem Soc* 138:1481
12. Yahiro H, Baba Y, Eguchi K, Arai H (1988) *J Electrochem Soc* 135:2077
13. Wachsman ED, Jayaweera P, Jiang N, Lowe DM, Pound BG (1997) *J Electrochem Soc* 144:233
14. Tsukamoto K, Uchiyama F, Kaga Y, Ohno Y, Yanagisawa T, Monma A, Takahagi Y, Lain MJ, Nakajima T (1990) *Solid State Ionics* 40-41(2):1003
15. Budd KD, Payne DA (1984) *Mater Res Soc Symp Proc* 32:239
16. Park J-Y, Yoon H, Wachsman ED (2005) *J Am Ceram Soc* 88 (9):2402
17. Park J-Y (2001) M.S. Thesis, University of Florida, Gainesville, FL